CHAPTER IV

RESULTS AND DISCUSSION

1. Plasmid DNA and preparation of plasmid DNA

pEGFP-C2 was amplified in *Escherichia coli* and was prepared by alkaline lysis technique. The acquired pDNA was dissolved in RNase/DNase free water and was stored at 4°C. The purity of pDNA was evaluated by OD_{260}/OD_{280} ratio. These ratios of all batches of pDNA were higher than 1.8, therefore the pDNA was purified enough to be used as a reporter gene. And, the concentration of all batches of pDNA ranged from 31.615 to 46.930 μg/μl.

2. Preparation of chitosan-pDNA nanoparticles

The chitosan-pDNA nanoparticles were prepared using complex coacervation method. To study the effect of formulation variables on physical properties and transfection efficiency of the chitosan-pDNA nanoparticles, three variables were selected; medium of chitosan, medium of pDNA and N/P ratio. The previous study of Mao et al. (2001) concluded that the sodium sulfate concentration, in the range of 2.5-25 mM, had no significant impact on the average size of the nanoparticles. The chitosan solution at pH of 5-5.8 and a temperature of the solution above 50°C resulted in nanoparticles with the least aggregates. Moreover, the optimal concentration of chitosan and pDNA to form stable and uniform nanoparticles ranged from 50 to 400 μg/ml for chitosan and 40 to 80 μg/ml for DNA in the final product. Thus in this study, the pDNA was used with fixed concentration of 100 μg/ml in various medium of pDNA, while the chitosan concentration was varied from 27.34 to 382.79 μg/ml in the solution with pH 5.5 to yield selected N/P ratios. And, the nanoparticles were prepared at 55°C.

3. Effect of formulation variables on physical properties of chitosan-pDNA nanoparticles

3.1 Effect on particle size, PI and zeta potential of the nanoparticles

The particle size, PI and zeta potential of all formulations were shown in Table 1 in the form of mean±SD. Figure 4 shows that the particle size of the nanoparticles decreased from micron size to submicron size with increasing N/P ratio and finally decreased to constant value in the range of 102-278 nm. This result was agreed with the previous study of Mao et al. (2001), which the particle size decreased with increasing N/P ratio and became stable in the range of 100 to 250 nm.

For chitosan-pDNA nanoparticles formulated with chitosan in lactic acid (CSL nanoparticles) and chitosan in glycolic acid (CSG nanoparticles), large aggregates in micron size were formed at N/P ratios of 0.5:1 and 1:1. Then the particle size sharply decreased and became stable in nanosize at N/P ratio of 2:1. For the nanoparticles formulated with chitosan in acetic acid (CSA nanoparticles), the large aggregates in micron size were also formed at N/P ratio of 0.5:1 for and then the particle size sharply decreased to constant value in nanosize at N/P ratio of 1:1. These results indicated that the particle size of CSA nanoparticles sharply decreased and became stable in nanosize at N/P ratio lower than those of CSL and CSG nanoparticles. The results were attributed to the molecular weight and molecular structure of the acid. The molecular weight was 60.05, 76.05 and 90.08 g/mol for acetic acid, lactic acid and glycolic acid, respectively. And, the molecular structure of acetic acid and glycolic acid was linear, while that of lactic acid was branched. At low N/P ratio, the negative charge was excess and the structure of pDNA was large and complex. Therefore the anions from acid hindered the formation of chitosan and pDNA. The hindrance effect was dependent on the molecular weight and molecular structure of acid, the higher the molecular weight and molecular structure, the higher the hindrance effect. As a result, CSA nanoparticles were completely formed at N/P ratio lower than CSL and CSG nanoparticles. Although the molecular weight and molecular structure of lactic acid and glycolic acid were different, the particle size of CSL and CSG nanoparticles decreased to constant value in

Table 1 Particle size, PI and zeta potential of chitosan-pDNA nanoparticles (mean±SD, n=3)

acid type	N/P ratio	sodium sulfate			sodium chloride			water		
		size (nm)	PI	zeta potential (mV)	size (nm)	PI	zeta potential (mV)	size (nm)	PI	zeta potential (mV)
acetic acid	0.5:1	12420.0±3147.6	0.52±0.42	-5.24±0.12	18866.7±4908.5	0.79±0.37	-4.21±0.73	17533.3±5616.4	0.75±0.44	-7.28±0.41
	1:1	232.0±6.0	0.31±0.04	10.73±0.15	188.7±1.5	0.31±0.02	21.50±0.76	202.7±3.0	0.34±0.00	17.57±0.35
	2:1	196.7±3.2	0.37±0.02	11.70±0.46	180.7±9.7	0.28±0.03	24.20±0.87	154.0±0.0	0.30±0.03	24.30±1.06
	3:1	187.0±4.0	0.30±0.02	11.63±0.71	181.3±4.2	0.31±0.05	23.30±0.87	156.7±5.0	0.34±0.05	22.07±1.20
	5:1	180.0±6.9	0.24±0.03	10.80±0.35	168.3±2.5	0.32±0.02	16.57±2.14	145.3±2.3	0.36±0.02	17.93±0.57
	7:1	212.7±7.8	0.26±0.01	12.20±0.72	178.3±1.5	0.32±0.01	16.50±1.15	150.0±2.0	0.37±0.02	19.17±1.36
lactic acid	0.5:1	25233.3±2936.6	0.43±0.49	-8.77±0.34	19300.0±5645.4	0.44±0.49	-9.66±0.50	12416.7±4431.8	0.35±0.22	-13.97±1.93
	1:1	22100.0±2116.6	0.28±0.10	2.43±0.68	31833.3±10607.7	0.22±0.21	8.29±0.60	30233.3±7518.2	0.61±0.46	0.52±0.52
	2:1	169.0±2.7	0.29±0.01	13.00±0.87	140.3±0.6	0.31±0.04	24.93±0.42	167.0±2.00	0.30±0.06	25.47±0.57
	3:1	148.7±6.7	0.28±0.02	7.70±1.15	278.0±7.0	0.35±0.04	29.03±1.00	208.0±2.65	0.35±0.01	22.37±1.63
	5:1	179.3±7.8	0.32±0.01	13.40±0.85	147.3±1.5	0.36±0.01	27.67±0.55	173.0±2.65	0.44±0.02	20.13±3.27
	7:1	131.0±1.0	0.20±0.02	14.47±0.85	158.3±4.9	0.51±0.02	33.53±0.95	135.0±6.08	0.38±0.01	27.30±2.44
glycolic acid	0.5:1	15766.7±3611.6	0.38±0.20	-10.63±0.68	21933.3±9141.9	0.79±0.36	-6.85±1.07	31466.7±11762.8	0.68±0.56	-10.19±0.67
	1:1	19333.3±7100.9	0.45±0.48	9.15±0.56	19266.7±2315.9	0.13±0.06	13.60±0.40	28033.3±7145.9	0.68±0.56	9.52±0.51
	2:1	217.3±1.2	0.34±0.01	13.57±0.29	136.3±2.9	0.27±0.03	27.50±0.10	119.3±2.3	0.32±0.01	27.10±1.31
	3:1	242.7±6.0	0.20±0.01	14.50±0.61	230.3±4.5	0.28±0.05	23.83±2.19	122.0±6.0	0.26±0.02	25.60±0.46
	5:1	179.0±3.6	0.35±0.02	13.50±0.60	187.0±8.2	0.37±0.05	26.00±1.22	102.7±1.5	0.31±0.03	21.87±5.58
	7:1	176.0±6.6	0.31±0.02	13.40±0.40	148.0±6.1	0.37±0.01	29.13±0.57	104.0±1.0	0.29±0.03	28.57±2.51

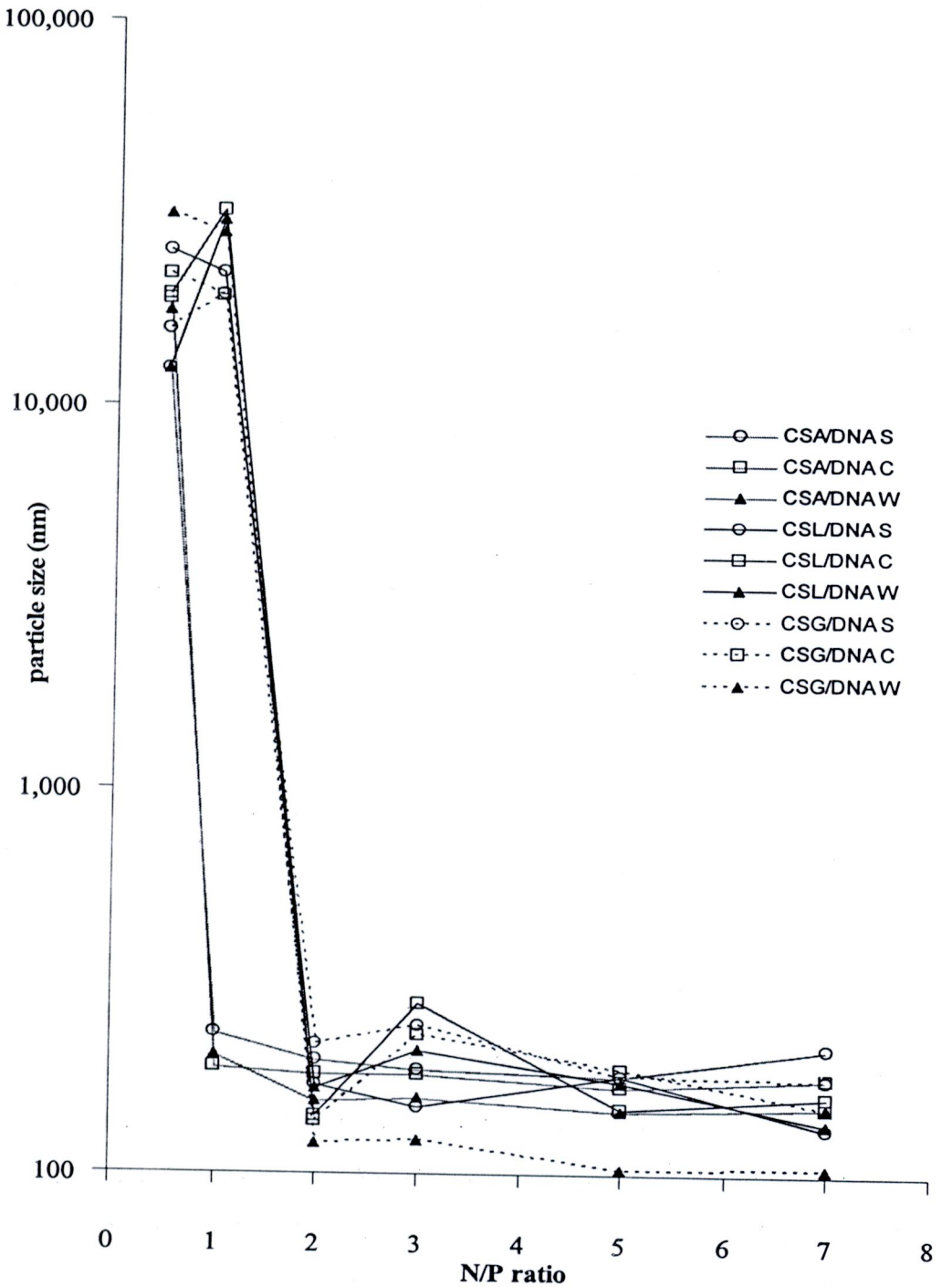

Figure 4 Particle size of chitosan-pDNA nanoparticles at varying N/P ratios. CSA, nanoparticles formulated with chitosan in acetic acid; CSL, nanoparticles formulated with chitosan in lactic acid; CSG, nanoparticles formulated with chitosan in glycolic acid; DNA S, nanoparticles formulated with pDNA in sodium sulfate; DNA C, nanoparticles formulated with pDNA in sodium chloride; DNA W, nanoparticles formulated with pDNA in water.

nanosize at the same N/P ratio. This result was the consequence of the selection of N/P ratio in this study. The molecular weight of glycolic acid was lower and the molecular structure was linear, so the hindrance effect was lower than lactic acid. As a result, CSG nanoparticles should completely form at N/P ratio lower than CSL nanoparticles and the N/P ratio should be between 1:1 and 2:1.

Of all media for chitosan, there was no tendency about which formulation possessed the largest particles size, while the CSL nanoparticles possessed the smallest size except the CSL nanoparticles formulated with pDNA in water. But the difference of particle size was very minute. The result indicated that the type of acid had an influence on the formation of the nanoparticles at low N/P ratio, while after the particle size sharply decreased and became stable in nanosize, the type of acid had little influence on the particle size of nanoparticles.

Of all media for pDNA, the nanoparticles formulated with pDNA in sodium sulfate (DNA S nanoparticles) possessed the largest particle size, while the nanoparticles formulated with pDNA in water (DNA W nanoparticles) possessed the smallest particle size except the CSL/DNA W nanoparticles. Complex coacervation method is a method of spontaneous phase separation that occurred when two oppositely charge polyelectrolytes were mixed together in an aqueous solution. The electrostatic interaction between the two opposite charges resulted in the separation of coacervate. The coacervating agent was used to increase the phase separation. Therefore the nanoparticles formulated with pDNA in coacervating agent, DNA S nanoparticles and the nanoparticles formulated with pDNA in sodium chloride (DNA C nanoparticles) had the particles size larger than DNA W nanoparticles. This result was agreed with the study of Romøren et al. (2003), in which particle size increased with the addition of coacervating agent. In this study, sodium sulfate and sodium chloride acted as coacervating agents. The difference between these two coacervating agents was the type and number of ion. Each ion has different hydrating power. Both sodium sulfate and sodium chloride have sodium ion, however sodium sulfate has two sodium ions, whereas sodium chloride has only one sodium ion. Moreover, sulfate ion from sodium sulfate has more hydrating power more chloride ion from sodium chloride according to the Hofmeister or lyotropic series (Bowman et al., 2006). As a result, sodium sulfate had a higher activity as coacervating agent than sodium chloride. Thus the particle size of DNA S

nanoparticles was larger than DNA C nanoparticles. The PI of the particle size of all formulation excepting the formulation that had the large aggregates was in the range of 0.20-0.51. The data indicated that the particle size of the chitosan-pDNA nanoparticles was in nanosize range with mostly narrow distribution.

Similar to the result of the particle size, Figure 5 shows that the zeta potential of the chitosan-pDNA nanoparticles increased from negative to positive with increasing N/P ratio and finally increased to constant value in the range of +7.70 to +33.53 mV. This increase was due to the additional density of positive charge from chitosan with the increase of N/P ratio. The similar results were observed in the previous studies of Erbacher et al. (1998) and Mao et al. (2001), which the zeta potential increased with increasing N/P ratio and became stable in the range of +12 to +35 mV. An initial negative value of the zeta potential was observed at N/P ratio of 0.5:1 of all formulation. For the CSL and CSG nanoparticles, the zeta potential was reached the plateau at N/P ratio of 2:1, while the zeta potential of CSA nanoparticles was reached the plateau at N/P ratio of 1:1. These results indicated that the zeta potential of the CSA nanoparticles reached the plateau at N/P ratio lower than those of CSL and CSG nanoparticles. The reason of these results was similar to the particle size as aforementioned.

Of all media for pDNA, the surface charge of the DNA S nanoparticles was markedly different from those of DNA C and DNA W nanoparticles, while the surface charge of DNA C and DNA W nanoparticles was nearly equal. The results were attributed to the difference of the valence of the medium of pDNA. Sodium sulfate has the highest valence of 2. Therèfore sodium sulfate had the most efficiency to shield the positive surface charge of the nanoparticles.

Of all media for chitosan, the CSA nanoparticles possessed the lowest surface charge, while the CSG nanoparticles possessed the highest surface charge except the CSG/DNA C nanoparticles. But the difference of surface charge was very minute. The result indicated that the type of acid had an influence on the formation of the nanoparticles at low N/P ratio, while after the particle size sharply decreased and became stable in nanosize, the type of acid had little influence on the surface charge of the nanoparticles.

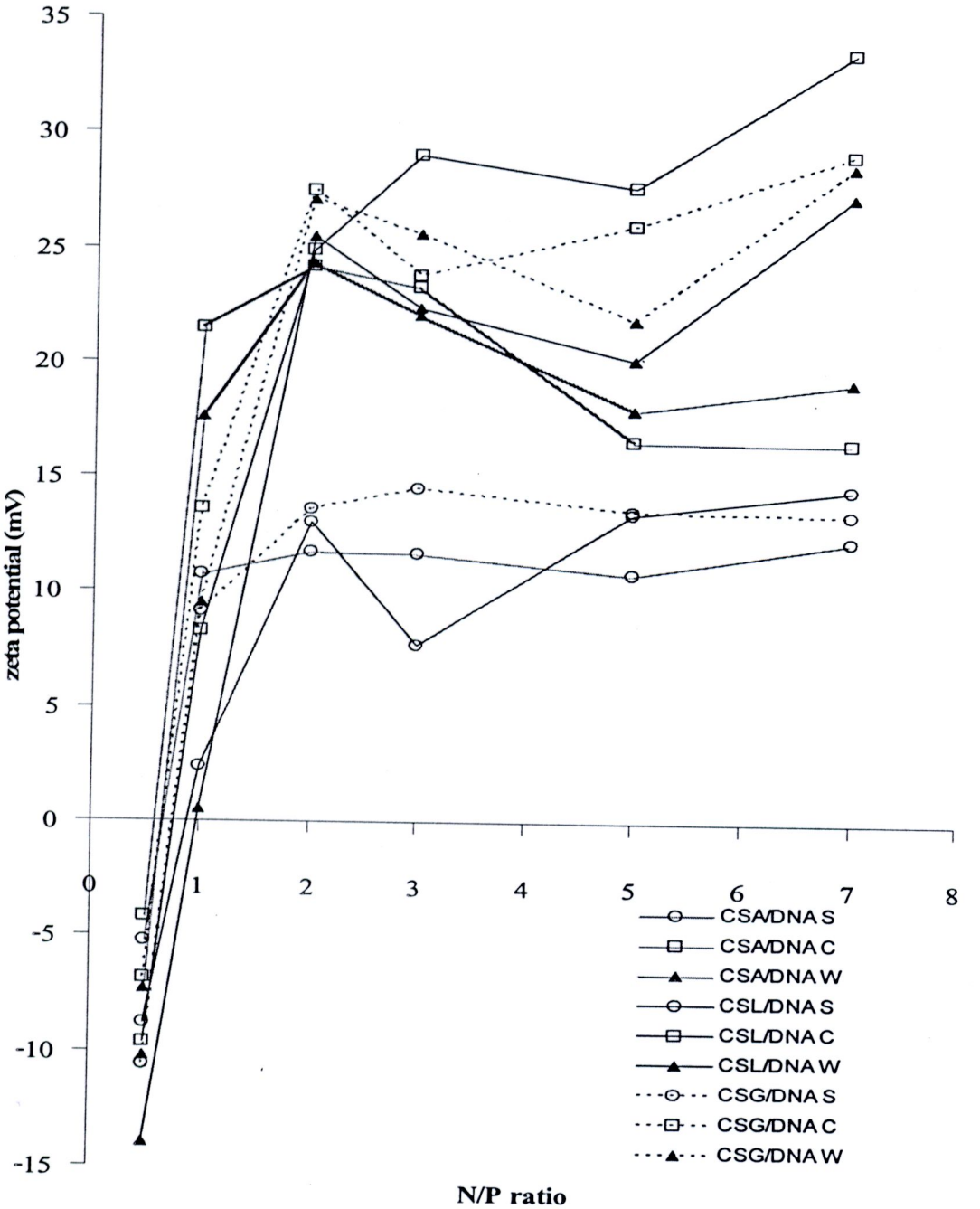

Figure 5 Zeta potential of chitosan-pDNA nanoparticles at varying N/P ratios. CSA, nanoparticles formulated with chitosan in acetic acid; CSL, nanoparticles formulated with chitosan in lactic acid; CSG, nanoparticles formulated with chitosan in glycolic acid; DNA S,

nanoparticles formulated with pDNA in sodium sulfate; DNA C, nanoparticles formulated with pDNA in sodium chloride; DNA W, nanoparticles formulated with pDNA in water.

Particle size and zeta potential were plotted against N/P ratio of chitosan-pDNA nanoparticles formulated with various chitosan in Figure 6-8. These plots of the CSL and CSG nanoparticles are shown in Figure 7 and 8. The plots showed that the particle size of the chitosan-pDNA nanoparticles was in micron size and the surface charge was negative at N/P ratio of 0.5:1. At this N/P ratio, the negative charge from pDNA was more than the positive charge from chitosan. As a result, the positive charge from chitosan was not enough to condense pDNA. Therefore, the binding of chitosan and pDNA was loose and the particle size of the nanoparticles was in micron size with the negative surface charge at N/P ratio of 0.5:1. At N/P ratio of 1:1, the particle size of the nanoparticles remained in micron size but the surface charge was slightly positive. This result attributed to the increasing of the positive charge from chitosan with the increase of N/P ratio. As a result, the surface charge was slightly positive. Although the increase of positive charge from chitosan was enough to condense the pDNA, the slightly positive charge was not enough to give the repulsion of each particle. Therefore the particles tended to accumulate together to form large aggregates.

At N/P ratio of 2:1, the particle size of the nanoparticles was in nanosize range and the surface charge was positive. At this N/P ratio, the particle size and zeta potential became stable that the particle size and surface charge were slightly changed with increasing N/P ratio, suggesting that all of the phosphate groups bound with chitosan and the residual chitosan remained unbound in the solution. Figure 6 shows the plots of particle size and zeta potential of the CSA nanoparticles. The result was similar to those of the CSL and CSG nanoparticles except the result at the N/P ratio of 1:1. At this ratio, the particle size and the surface charge of the nanoparticles became stable. The particle size was in nanosize range and the surface charge was positive. This suggested that the CSA nanoparticles had more efficiency to condense the pDNA than the CSL and CSG nanoparticles.

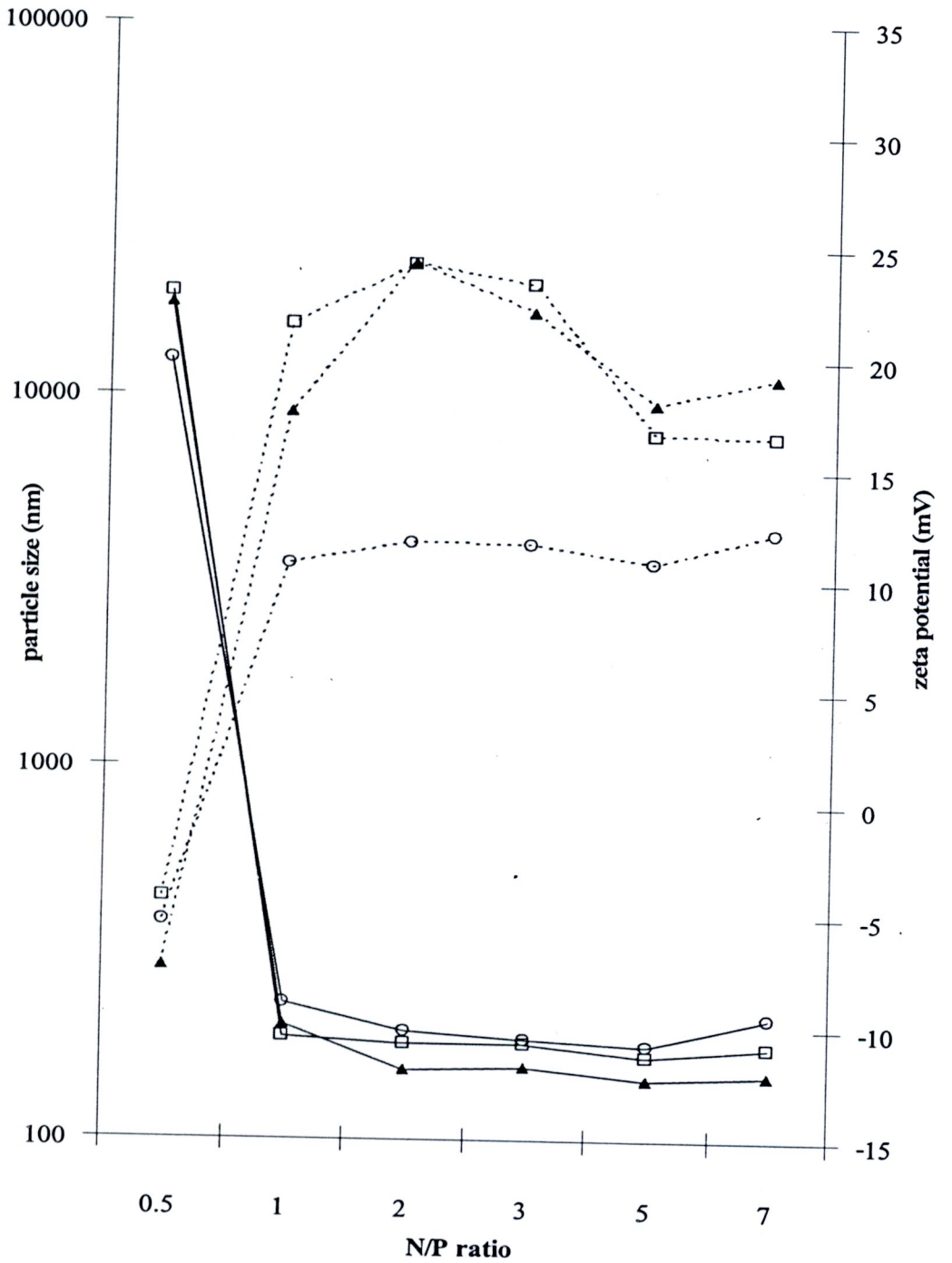

Figure 6 Particle size and zeta potential at varying N/P ratios of the CSA nanoparticles. (——) particle size; (------) zeta potential; (O) DNA S, nanoparticles formulated with pDNA in sodium sulfate; (□) DNA C, nanoparticles formulated with pDNA in sodium chloride; (▲) DNA W, nanoparticles formulated with pDNA in water.

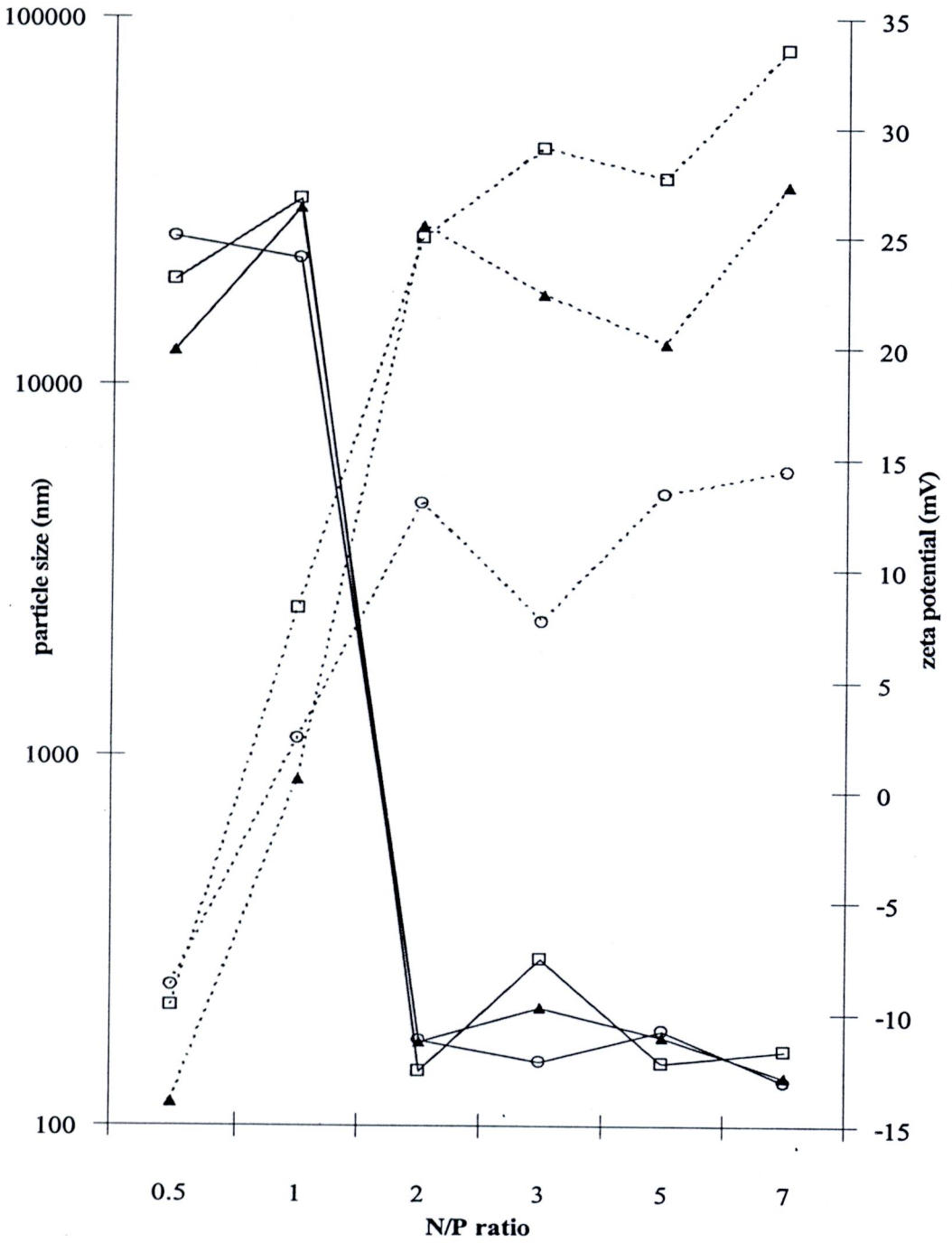

Figure 7 Particle size and zeta potential at varying N/P ratios of the CSL nanoparticles. (——) particle size; (------) zeta potential; (O) DNA S, nanoparticles formulated with pDNA in sodium sulfate; (□) DNA C, nanoparticles formulated with pDNA in sodium chloride; (▲) DNA W, nanoparticles formulated with pDNA in water.

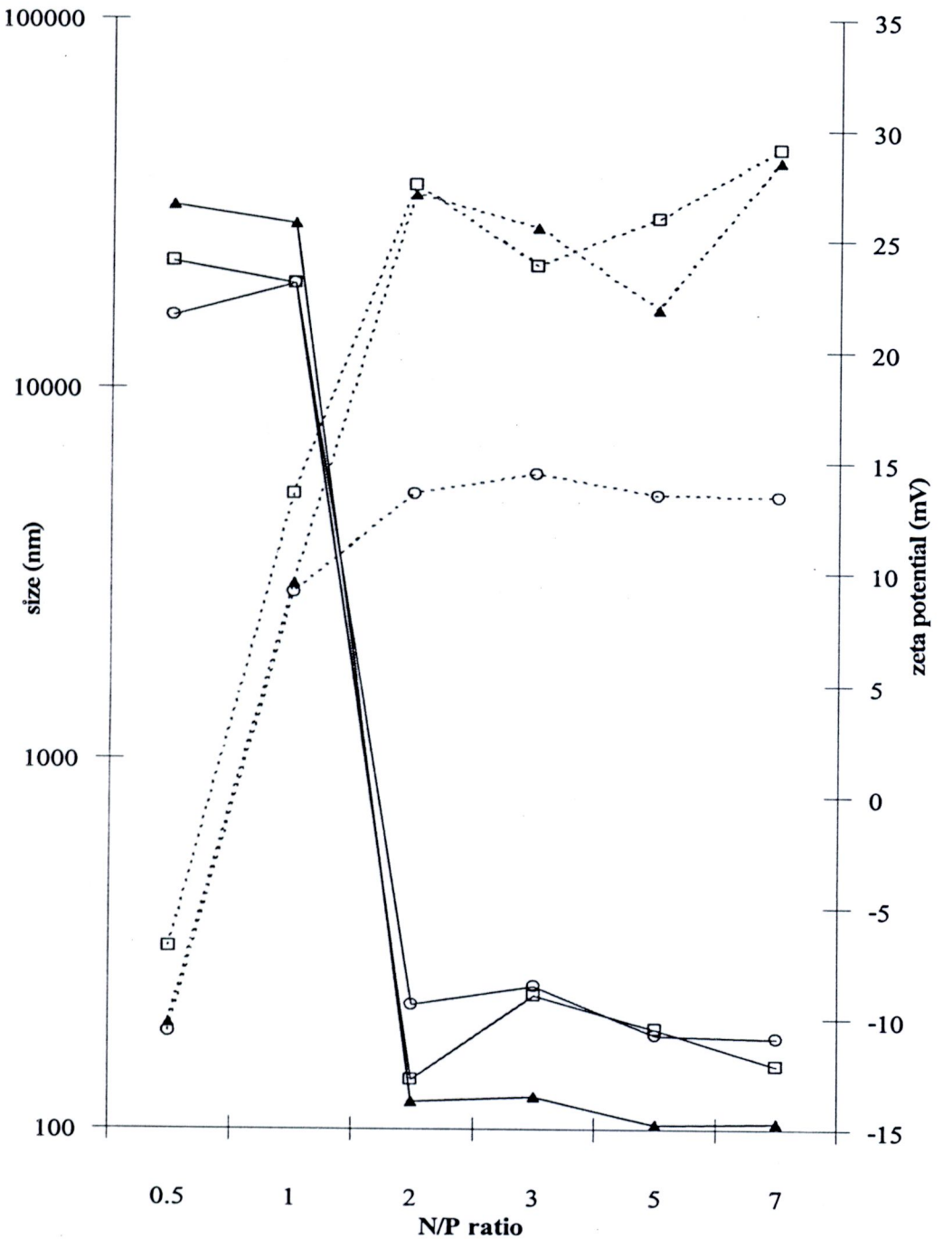

Figure 8 Particle size and zeta potential at varying N/P ratios of the CSG nanoparticles. (——) particle size; (------) zeta potential; (O) DNA S, nanoparticles formulated with pDNA in sodium sulfate; (□) DNA C, nanoparticles formulated with pDNA in sodium chloride; (▲) DNA W, nanoparticles formulated with pDNA in water.

From the particle size, PI and zeta potential of all formulations, it was found that the particle size and zeta potential of nanoparticles formulated at N/P ratio of 2:1 was in the range of constant value. As a result, the formulations at N/P ratio of 2:1 were selected for further study. And the CSA/DNA S nanoparticles formulated at N/P ratio of 3:1, 5:1 and 7:1 (3:1 CSA/DNA S nanoparticles, 5:1 CSA/DNA S nanoparticles and 7:1 CSA/DNA S nanoparticles) were selected for further study to examine the effect of N/P ratio on transfection efficiency.

3.2 Effect on morphology of the nanoparticles

The morphology of the nanoparticles was examined by transmission electron microscopy (TEM). TEM images of 5:1 CSA/DNA S, 2:1 CSA/DNA S, 2:1 CSA/DNA C and 2:1 CSA/DNA W nanoparticles, as representatives of all formulations, are shown in Figure 9-12, respectively. Almost all of the 5:1 CSA/DNA S, 2:1 CSA/DNA S and 2:1 CSA/DNA C nanoparticles (Figure 9-11) had spherical shape, while a few particles had rod shape. Figure 12 shows that 2:1 CSA/DNA W nanoparticles had particle fewer than those of other formulations and had spherical shape. The result was agreed with the shape of chitosan-pDNA nanoparticles from Mao et al. (2001) and MacLauhlin et al. (1998). Other shapes, donut and pretzel shape, were observed in the study from Erbacher et al. (1998). Aggregation of a few particles was observed in all represented formulations. The particle size was confirmed in the size range of 100 to 200 nm, which agreed with aforementioned particle size measurement from PCS.

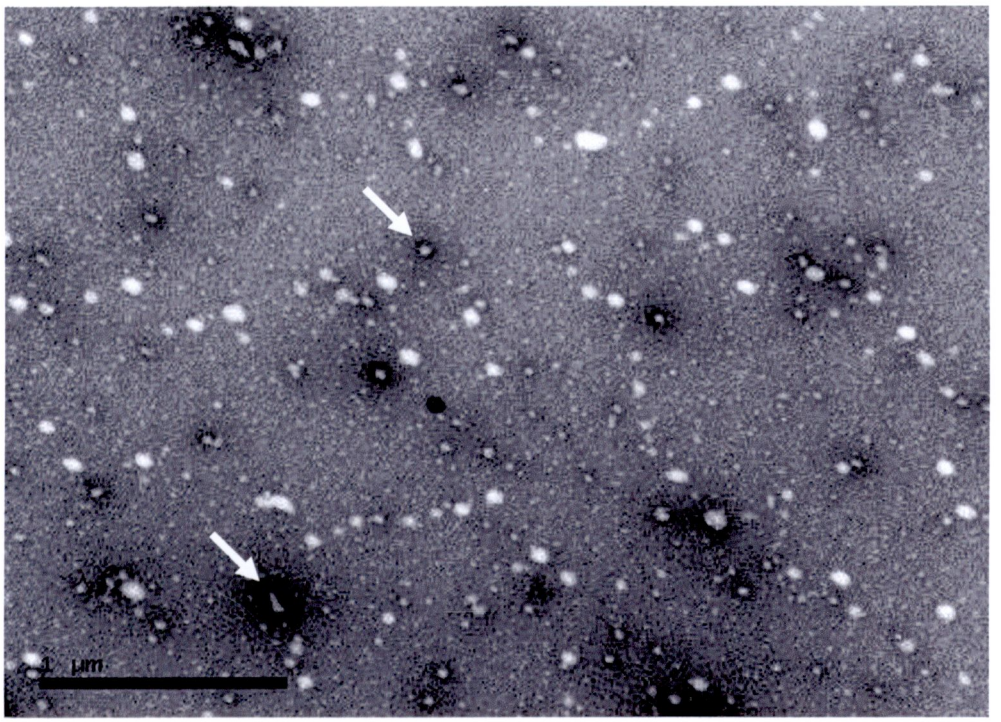

Figure 9 TEM image of 5:1 CSA/DNA S nanoparticles. Bar represents 1 µm. Total magnification is X39600.

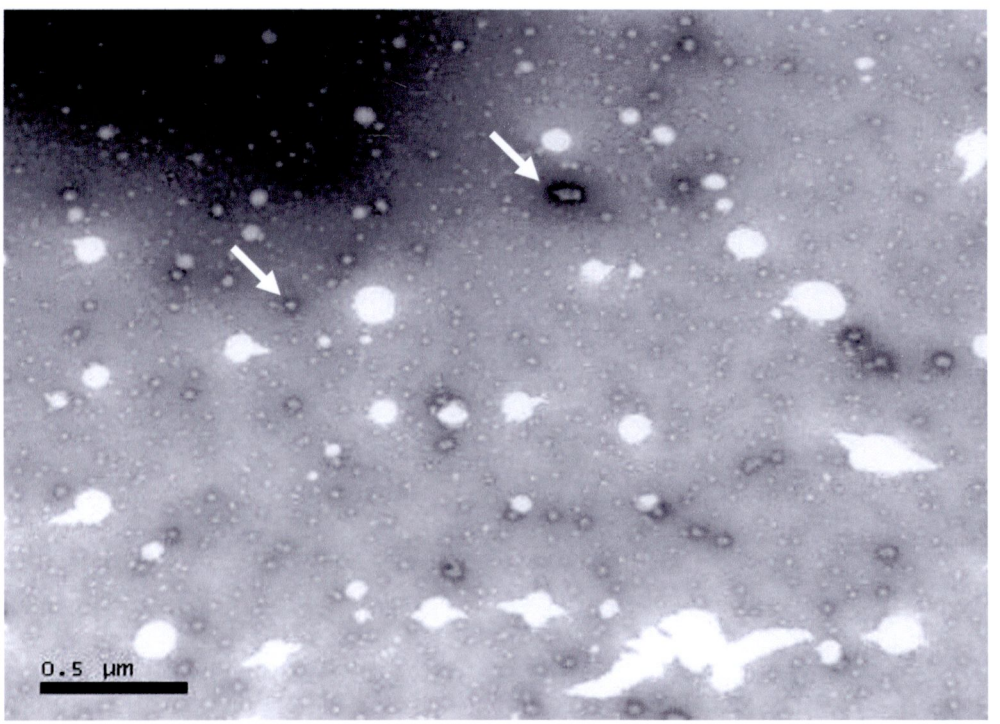

Figure 10 TEM image of 2:1 CSA/DNA S nanoparticles. Bar represents 0.5 µm. Total magnification is X47400.

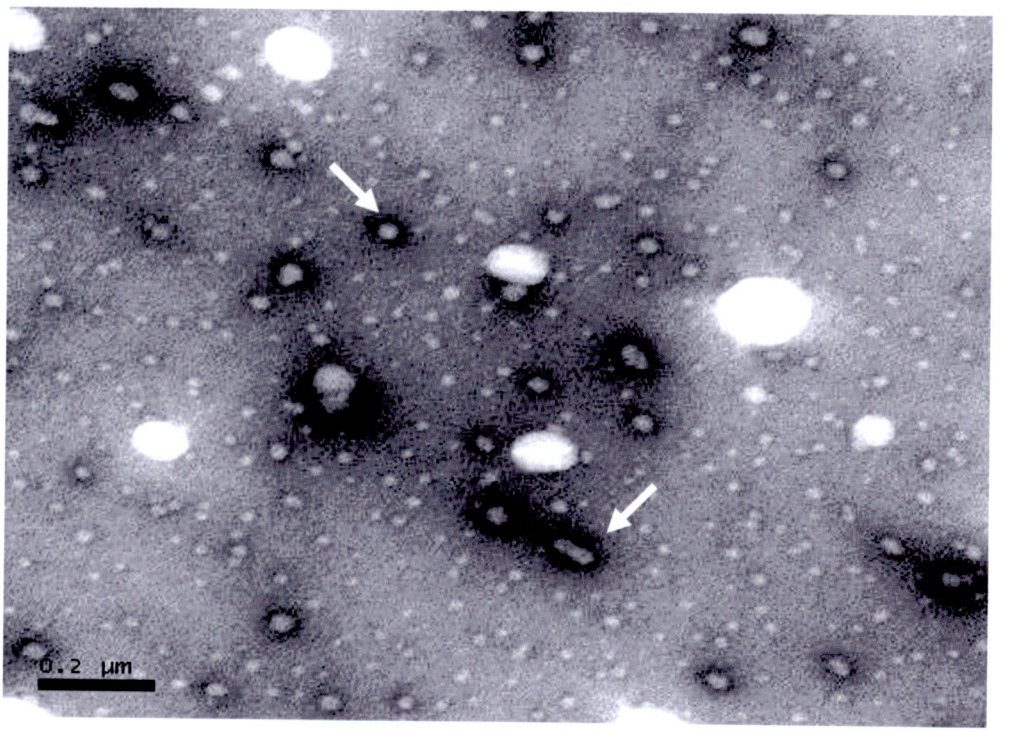

Figure 11 TEM image of 2:1 CSA/DNA C nanoparticles. Bar represents 0.2 µm. Total magnification is X94400.

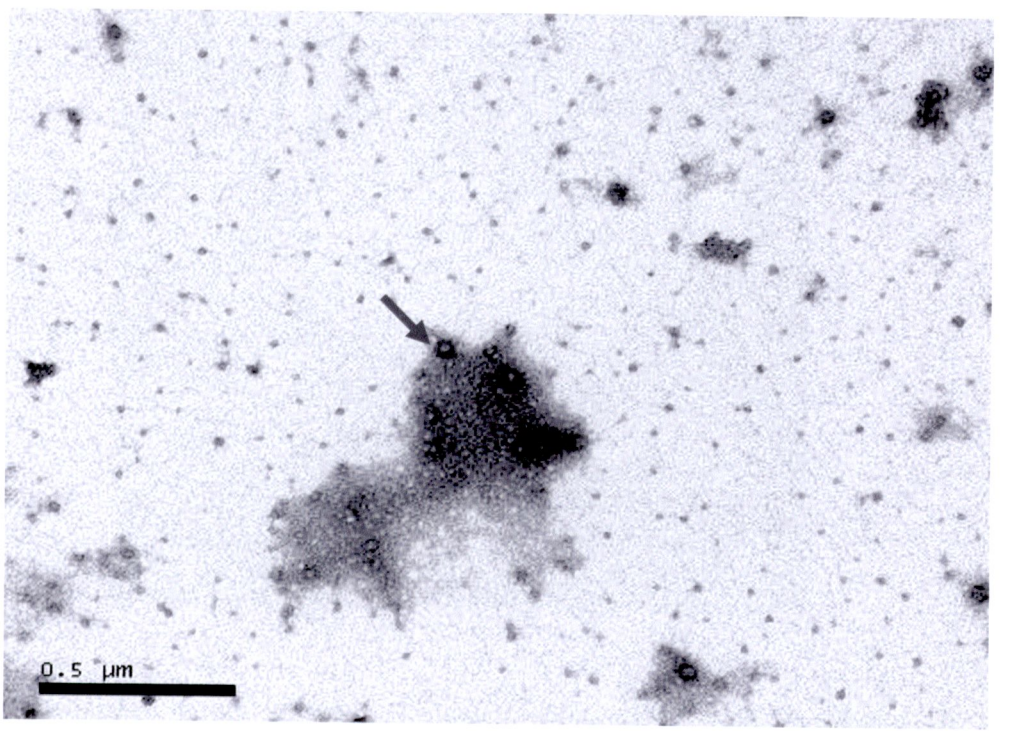

Figure 12 TEM image of 2:1 CSA/DNA W nanoparticles. Bar represents 0.5 µm. Total magnification is X63000.

4. Gel retardation assay

The nanoparticles formation was evaluated by using agarose gel electrophoresis. Figure 13 shows the electrophoretic mobility of naked pDNA and the CSA/DNA S nanoparticles at N/P ratios of 0.5:1, 1:1, 2:1, 3:1, 5:1 and 7:1. The naked pDNA lane showed the pDNA band, while nanoparticles lanes showed that the nanoparticles were completely retarded within the gel loading well for all N/P ratios. From the result of particle size and zeta potential of CSA/DNA S nanoparticles, the nanoparticles was in micron size at N/P ratio of 0.5:1. Although at this ratio the positive charge of chitosan was not enough to withdraw pDNA to submicron size, the positive charge was enough to retard pDNA from migration in gel electrophoresis. At other N/P ratio, the positive charge can condense pDNA and formed complete complexes.

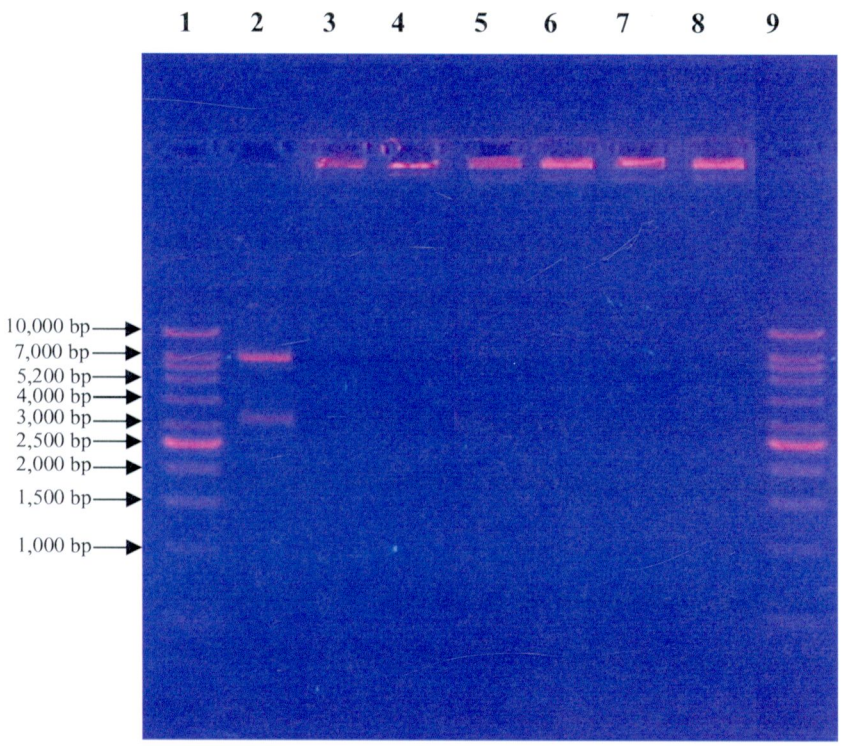

Figure 13 Electrophoretic mobility analysis of naked pDNA and CSA/DNA S nanoparticles at varying N/P ratios. Lane (1 and 9) 1 kb DNA ladder; lane (2) naked pDNA; lane (3-8) CSA/DNA S nanoparticles at N/P ratios of 0.5:1, 1:1, 2:1, 3:1, 5:1 and 7:1, respectively.

5. Protection effect of nanoparticles to pDNA

There are 3 procedures for chitosan digestion; digestion 1, digestion 2 and digestion 3. Figure 14 shows the electrophoretic mobility of 2:1 CSA/DNA S nanoparticles following chitosan digestion using digestion 1 (a), digestion 2 (b) and digestion 3 (c). Lane 2 showed pDNA band consisted of upper band (approximately 3 kb) and lower band (approximately 6 kb) of naked pDNA in water. Lane 3 revealed the band of naked pDNA in water after incubated at 37°C for a period of time of each digestion. The pDNA band of Lane 3 of figure 14 (a and b) was not different from lane 2, while that of figure 14 (c) was lighter compared to lane 2. This indicated that the condition of digestion 1 and 2, at 37°C for 4 hours, did not affect pDNA, while the condition of digestion 3, at 37°C for 12 hours, affected the pDNA.

Lane 4 showed pDNA band of naked pDNA incubated with chitosanase and lysozyme in the concentration of each digestion followed by incubation at 37°C for a period of time of each digestion. The pDNA band of lane 4 of all digestions differed from those of naked pDNA in lane 2. The pDNA band of lane 4 (a and b) had only upper band and pDNA was partially retarded in the well, while that of lane 4 (c) was completely retarded in the well. This indicated that addition of chitosanase and lysozyme influenced the electrophoretic mobility pDNA. The result attributed to the association of lysozyme with pDNA and prevented the pDNA from moving under electrophoresis. The association occurred because of the similarity of structure between lysozyme and histones, acted as spools for DNA molecule and enabled the compaction necessary to fit the large DNA molecule inside cell nucleus, according to the study of Steinrauf et al. (1999).

Lane 5 showed electrophoretic mobility of the nanoparticles incubated with chitosanase and lysozyme in the concentration of each digestion followed by incubation at 37°C for a period of time of each digestion. The pDNA band of lane 5 (a and b) had only upper band and pDNA was partially retarded in the well, however, the pDNA band of lane 5 by digestion 2 (b) looked like naked pDNA from lane 2, both intensity and position, more than that of lane 5 by digestion 1 (a), while that of lane 5 (c) was completely retarded in the well. The result indicated that, in this study, chitosan digestion by these 3 experimental conditions was not complete.

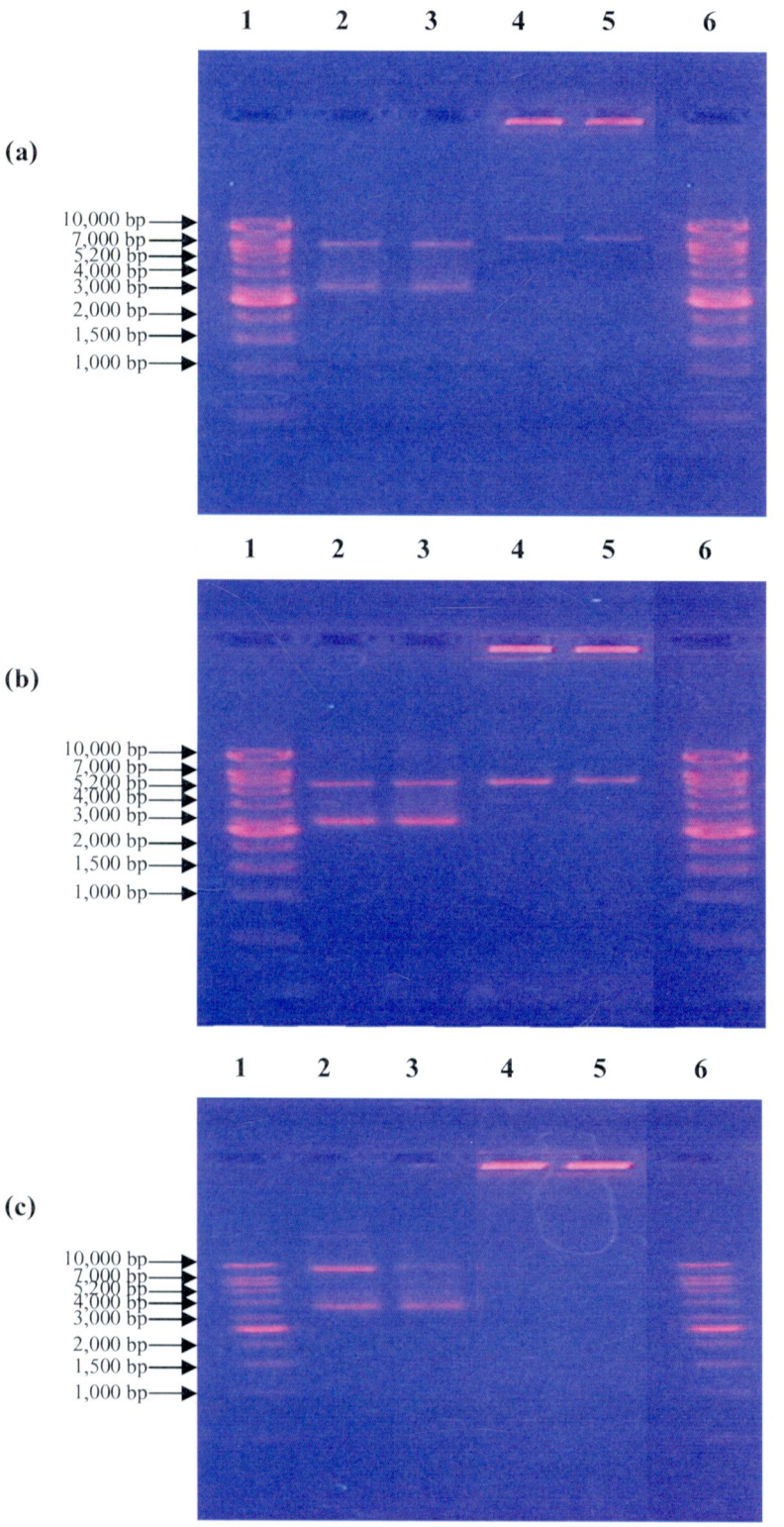

Figure 14 Electrophoretic mobility analysis of the digestion of 2:1 CSA/DNA S nanoparticles with digestion 1 (a), digestion 2 (b) and digestion 3 (c). Lane (1 and 6) 1 kb DNA ladder; lane (2) naked pDNA; lane (3) pDNA+condition of each digestion; lane (4) pDNA+chitosan digestion; lane (5) 2:1 CSA/DNA S nanoparticles+chitosan digestion in their condition.

Therefore, digestion 2 was selected to use in the protection study and the naked pDNA incubated with chitosanase and lysozyme followed digestion 2 at 37°C for 4 hours was used as a control.

The stability of chitosan-pDNA nanoparticles from deoxyribonuclease degradation was examined using DNase I. Naked pDNA 1 μg and chitosan-pDNA nanoparticles containing 1 μg of pDNA were incubated with 0.25 units of DNase I. Then, these nanoparticles were subjected to chitosanase and lysozyme digestion at a final concentration of 0.15U/ml and 15U/ml, respectively. The nanoparticles formulated at N/P ratio of 2:1 and 3:1, 5:1 and 7:1 CSA/DNA S nanoparticles were selected in this study. The electrophoretic mobility of nanoparticles from selected formulation following DNase I digestion and chitosan digestion is shown in figure 15 and 16. Lane 2 of both figures showed pDNA band consisted of upper and lower band of naked pDNA in water. Lane 3 of both figures revealed the band of pDNA after digested by DNase I. Lane 3 had no band of pDNA, indicated that DNase I used in this study could completely digested pDNA.

Lane 4 of both figures showed pDNA band of naked pDNA followed chitosan digestion. The pDNA band of lane 4 had only upper band and pDNA was partially retarded in the well. This lane was used as a control to determine whether the selected formulation could protect pDNA from DNase I degradation. Lane 5 of both figures showed the electrophoretic mobility of 2:1 CSA/DNA S nanoparticles. The pDNA band of lane 5 was at the well, indicated that pDNA was completely retarded in the well.

Lane 6 of figures 15 showed pDNA band of 2:1 CSA/DNA S nanoparticles followed chitosan digestion. The pDNA band of lane 4 had only upper band and pDNA was retarded in the well. Lane 7 of figure 15 showed the electrophoretic mobility of 2:1 CSA/DNA S nanoparticles after digested by DNase I. The pDNA band of lane 7 was at well with comparable intensity with lane 5, demonstrated that nanoparticles might be could protect pDNA from DNase I digestion.

Lane 8-11 of figure 15 revealed the electrophoretic mobility of CSA/DNA S nanoparticles at N/P ratio of 2:1, 3:1, 5:1 and 7:1 following DNase I and chitosan digestion, respectively. Lane 6-14 of figure 16 showed the electrophoretic mobility of the nanoparticles formulated at N/P ratio of 2:1 following DNase I and chitosan digestion, respectively. These lanes showed the pDNA band similarly to that of lane 4, the control. This suggested that all selected formulations could render protection to pDNA. It was probably that complexation induced changes in tertiary structure causing steric hindrance as described by Richardson et al. (1999).

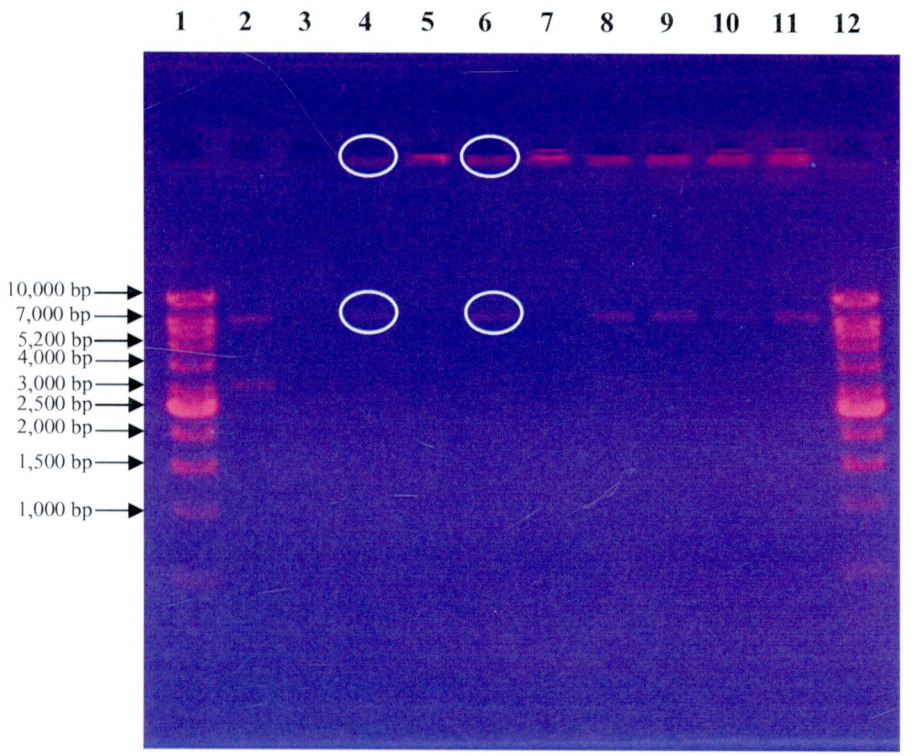

Figure 15 Electrophoretic mobility analysis of 2:1, 3:1, 5:1 and 7:1 CSA/DNA S nanoparticles following DNase I digestion and chitosan digestion. Lane (1 and 12) 1 kb DNA ladder; lane (2) naked pDNA; lane (3) pDNA+DNase I; lane (4) pDNA+chitosan digestion; lane (5) 2:1 CSA/DNA S nanoparticles; lane (6) 2:1 CSA/DNA S nanoparticles+chitosan digestion; lane (7) 2:1 CSA/DNA S nanoparticles+DNase I; lane (8) 2:1 CSA/DNA S nanoparticles+DNase I+chitosan digestion; lane (9) 3:1 CSA/DNA S nanoparticles+DNase I+chitosan digestion; lane (10) 5:1 CSA/DNA S nanoparticles+DNase I+chitosan digestion; lane (11) 7:1 CSA/DNA S nanoparticles+DNase I+chitosan digestion.

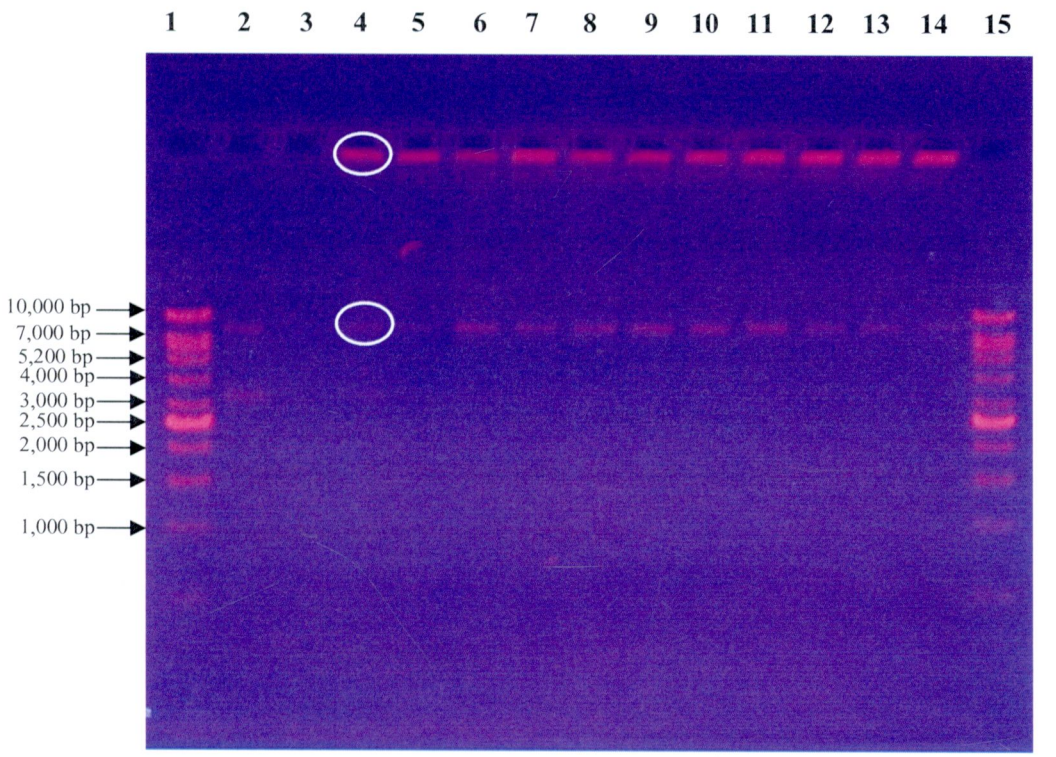

Figure 16 Electrophoretic mobility analysis of the nanoparticles formulated at N/P ratio of 2:1 following DNase I digestion and chitosan digestion. Lane (1 and 15) 1 kb DNA ladder; lane (2) naked pDNA; lane (3) pDNA+DNase I; lane (4) pDNA+chitosan digestion; lane (5) 2:1 CSA/DNA S nanoparticles; lane (6) 2:1 CSA/DNA S nanoparticles+DNase I+chitosan digestion; lane (7) 2:1 CSA/DNA C nanoparticles+DNase I+chitosan digestion; lane (8) 2:1 CSA/DNA W nanoparticles+DNase I+chitosan digestion; lane (9) 2:1 CSL/DNA S nanoparticles+DNase I+chitosan digestion; lane (10) 2:1 CSL/DNA C nanoparticles+DNase I+chitosan digestion; lane (11) 2:1 CSL/DNA W nanoparticles+DNase I+chitosan digestion; lane (12) 2:1 CSG/DNA S nanoparticles+DNase I+chitosan digestion; lane (13) 2:1 CSG/DNA C nanoparticles+DNase I+chitosan digestion; lane (14) 2:1 CSG/DNA W nanoparticles+DNase I+chitosan digestion.

6. Effect of formulation variables on *in vitro* transfection efficiency of chitosan-pDNA nanoparticles

The chitosan-pDNA nanoparticles from the formulations formulated at N/P ratio of 2:1 and 3:1, 5:1 and 7:1 CSA/DNA S nanoparticles were incubated with HeLa cells to investigate the effect of formulation variables on *in vitro* transfection efficiency. Naked pDNA was used as a negative control, while Lipofectamine™-pDNA complexes were used as a positive control. Each well of HeLa cells was incubated with pDNA or nanoparticles contained 1 μg of pDNA for 4 hours at 37°C in a humidified 5% CO_2 incubator and was analyzed 24 hours after transfection. Analysis of the transfection efficiency used 2 methods.

6.1 Fluorescence microscopy

After transfection, the cells were directly viewed under a fluorescence microscope to estimate the transfection efficiency. Figure 17 shows the image of HeLa cells under fluorescence microscope after transfection. There was no signal of fluorescence in HeLa cells incubated with naked pDNA as shown in figure 17 (a). In figure 17 (c), the fluorescence signals were visible in the HeLa cells incubated with Lipofectamine™-pDNA complexes. Some signals of fluorescence were visible in the HeLa cells incubated with 5:1 CSA/DNA W nanoparticles, but the fluorescence intensity was lower than those of positive control as shown in figure 17 (b). The HeLa cells from all formulations formulated at N/P ratio of 2:1 and 3:1, 5:1 and 7:1 CSA/DNA S nanoparticles were directly viewed under fluorescence microscope. The signals of fluorescence of HeLa cells of other formulations except 5:1 CSA/DNA S nanoparticles were very low. Therefore their images were not shown. In addition, from the image under microscope, the change of HeLa cells incubated with Lipofectamine™-pDNA complexes was observed. Some HeLa cells detached from the well and had rough edge, while HeLa cells incubated with chitosan-pDNA nanoparticles were not changed. Using the fluorescence microscope was the estimation of transfection efficiency. Thus, the flow cytometry was used to quantitatively assay the transfection efficiency of selected formulations.

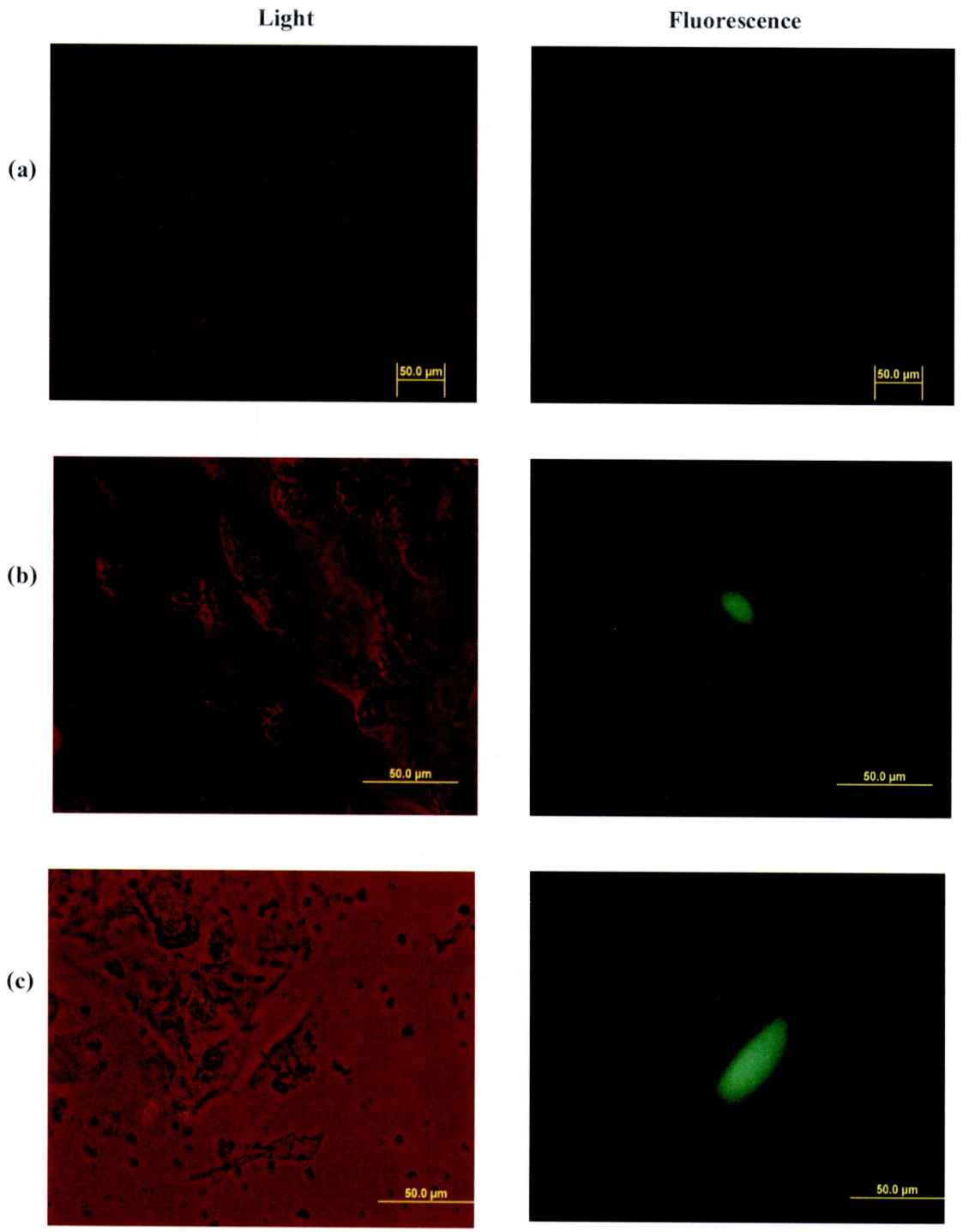

Figure 17 The image of HeLa cells under fluorescence microscope after incubated with **(a)** naked pDNA **(b)** 5:1 CSA/DNA S nanoparticles and **(c)** Lipofectamine™-pDNA nanoparticles.

6.2 Flow cytometry

In vitro transfection efficiency in HeLa cells was quantitatively assessed by flow cytometry. The transfection efficiency of chitosan-pDNA nanoparticles formulated at N/P ratio of 2:1 was shown as percentage of positive cells in Figure 18. The percentages of positive cells of naked pDNA in all medium were nearly zero, while that of the positive control was 14.60. The percentage of positive cells of positive control was significantly different from negative control ($P<0.05$).

The transfection efficiencies of all nanoparticles formulated at N/P ratio of 2:1 were higher than that of naked pDNA. The percentage of positive cells of the 2:1 CSA/DNA W, 2:1 CSL/DNA W and 2:1 CSG/DNA W nanoparticles (orange bars) were significantly different from naked pDNA but not significantly different from positive control ($P>0.05$), while those of 2:1 CSL/DNA C, 2:1 CSG/DNA S and CSG/DNA C nanoparticles (yellow bars) were not significantly different from both naked pDNA and positive control. And the percentage of positive cells of 2:1 CSA/DNA S, 2:1 CSA/DNA C and 2:1 CSL/DNA S nanoparticles (green bars) were not significantly different from naked pDNA but significantly different from positive control.

The results demonstrated that DNA W nanoparticles exhibited the most transfection efficiency followed by that of DNA C nanoparticles and DNA S nanoparticles, respectively. These results were attributed to the medium of pDNA or the coacervating agent. The anion from medium of pDNA hindered the attachment of the nanoparticles to HeLa cells. Therefore DNA W nanoparticles, which had no anion, had the most transfection efficiency. The two valences of sulfate anion provided more hindrance effect than chloride ion, which had only one valence. Thus transfection efficiency of DNA C nanoparticles was more than that of DNA S nanoparticles. The results were agreed with the study of Romøren et al. (2003). Romøren et al. concluded that the addition of a coacervating agent, sodium sulfate, up to 100 mM in the plasmid solution was not important to the transfection efficiency of the nanoparticles.

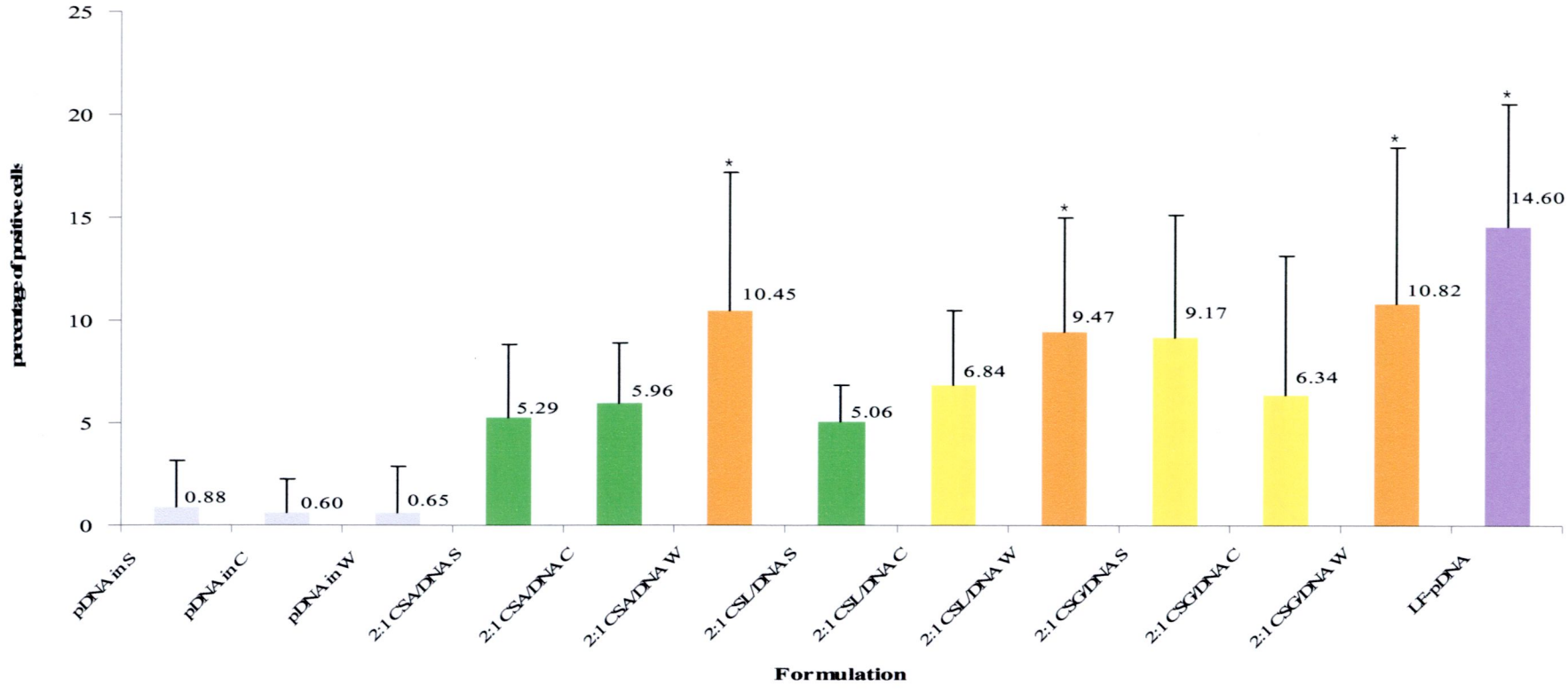

Figure 18 *In vitro* transfection efficiency of chitosan-pDNA nanoparticles formulated at N/P ratio of 2:1 was shown as percentage of positive cells (mean±SD, n=3) compared with negative control and positive control. Differences values were statistically significant (*P<0.05). CSA, nanoparticles formulated with chitosan in acetic acid; CSL, nanoparticles formulated with chitosan in lactic acid; CSG, nanoparticles formulated with chitosan in glycolic acid; DNA S, nanoparticles formulated with pDNA in sodium sulfate; DNA C, nanoparticles formulated with pDNA in sodium chloride; DNA W, nanoparticles formulated with pDNA in water; LF-pDNA, Lipofectamine™-pDNA complexes; S, sodium sulfate; C, sodium chloride; W, water.

The percentage of positive cells of the 2:1, 3:1, 5:1 and 7:1 CSA/DNA S nanoparticles is shown in figure 19. The percentage of positive cells of the 5:1 CSA/DNA S (orange bar) was significantly different from naked pDNA but not significantly different from positive control, while those of 3:1 CSA/DNA S and 7:1 CSA/DNA S nanoparticles (yellow bars) were not significantly different from those of both naked pDNA and positive control. And the percentage of positive cells of 2:1 CSA/DNA S nanoparticles (green bar) was not significantly different from negative control but significantly different from positive control. It seemed that the transfection efficiency had a tendency to increase with the increasing of N/P ratio for the 2:1 CSA/DNA S nanoparticles, 3:1 CSA/DNA S nanoparticles and 5:1 CSA/DNA S nanoparticles. This result indicated that the transfection efficiency was dependent on N/P ratio. Endosomal escape of the nanoparticles was one of the rate-limiting step in gene delivery. The enzymatic degradation of chitosan produced oligo- and monosaccharide, that increased the osmolarity of the endosomes. The increase induced the water influx, swelling and finally the rupture of the membrane of endosome and release of the plasmid. Increasing N/P ratio was followed by the increase of chitosan concentration in the nanoparticles. Higher amounts of chitosan in the nanoparticles led to a higher osmotic pressure in the endosome and as a result, the efficiency of plasmid release increased. The results were in agreement with the study of Romøren et al. (2003), which reported that nanoparticles formulated at N/P ratio of 0.5:1 hardly transfect EPC cells, while nanoparticles formulated at N/P ratio of 2:1 and 5:1 resulted in expression of reporter gene and concluded that the N/P ratio was strongly positive correlated to the transfection efficiency.

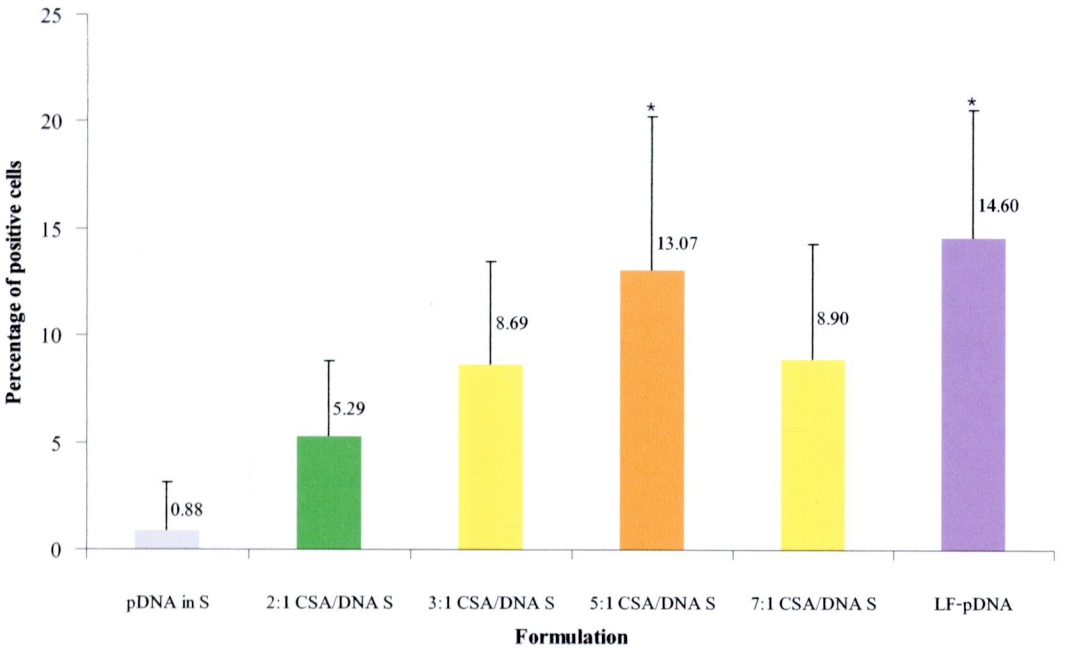

Figure 19 *In vitro* transfection efficiency of the 2:1, 3:1 5:1 and 7:1 CSA/DNA S nanoparticles was shown as percentage of positive cells (mean±SD, n=3) compared with negative control and positive control. Differences values were statistically significant (*P<0.05). CSA, nanoparticles formulated with chitosan in acetic acid; DNA S, nanoparticles formulated with pDNA in sodium sulfate; LF-pDNA, Lipofectamine™-pDNA nanoparticles; S, sodium sulfate.

7. Cell viability

Cell viability tests were evaluated by MTT assay to evaluate the potential of chitosan as a safe vector for gene delivery. The chitosan-pDNA nanoparticles, Lipofectamine™-pDNA complexes and various concentration of chitosan in all media of chitosan were incubated with HeLa cells for 72 hours. The concentration of chitosan was in the range of 2-25 μg/ml, which covered the concentration of chitosan used in the *in vitro* transfection efficiency study. The selected formulation were nanoparticles formulated at N/P ratio of 2:1 and 3:1, 5:1 and 7:1 CSA/DNA S nanoparticles. The cells treated with only DMEM was a control, used in the calculation of % cell viability and the cells treated with naked pDNA were a negative control.

7.1 Cell viability of HeLa cells incubated with various concentration of chitosan and Lipofectamine™ Reagent

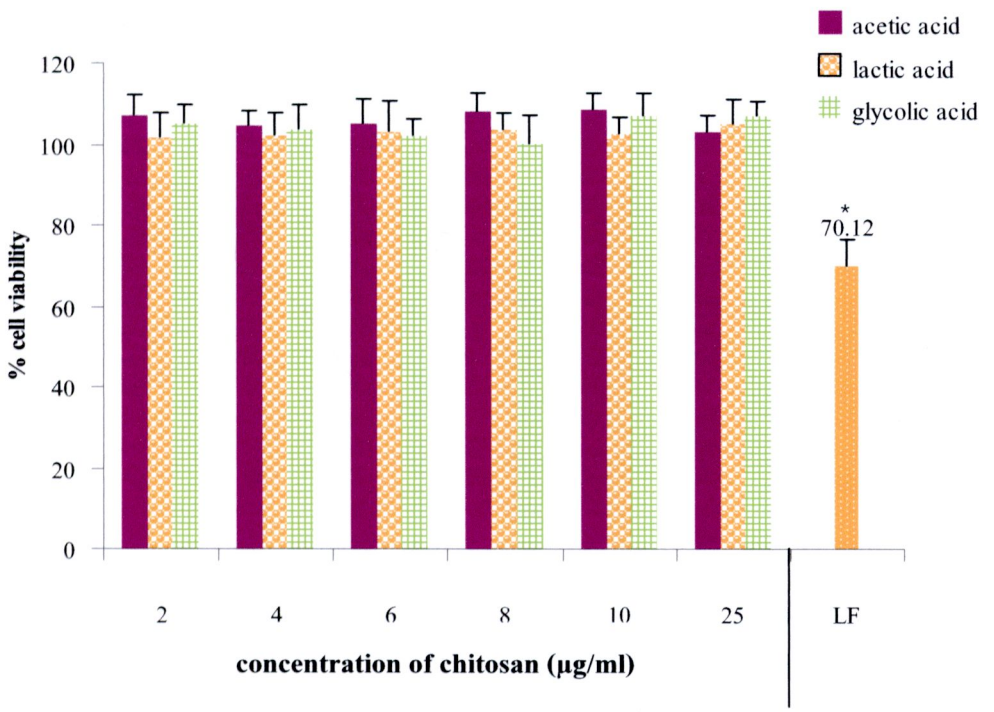

Figure 20 % Cell viability of HeLa cells incubated with various concentration of chitosan and Lipofectamine™ Reagent (mean±SD, n=3). Differences values were statistically significant (*P<0.05). LF, Lipofectamine™ Reagent.

Figure 20 shows that % cell viability of HeLa cells incubated with chitosan concentration in the range of this study was nearly 100% for all media of chitosan. The result indicated that chitosan in the concentration range of 2-25 µg/ml, which covered the concentration of chitosan used in the *in vitro* transfection efficiency study did not affect the viability of HeLa cells, while % cell viability of HeLa cells incubated with Lipofectamine™ reagent was 70.12%, which was significantly different from each other. The result indicated that chitosan in the concentration range used in this study was safer than Lipofectamine™ reagent. Chitosan is a naturally occurring polysaccharide produced by alkaline deacetylation of chitin extracted mainly from crustaceous shells. Chitosan is known as a biocompatible, biodegradable and non-toxic material

with low immunogenicity (Dodane and Vilivalam, 1998). Therefore chitosan is potential candicate as a safe vector for gene delivery.

7.2 Cell viability of HeLa cells incubated with the medium of selected formulations

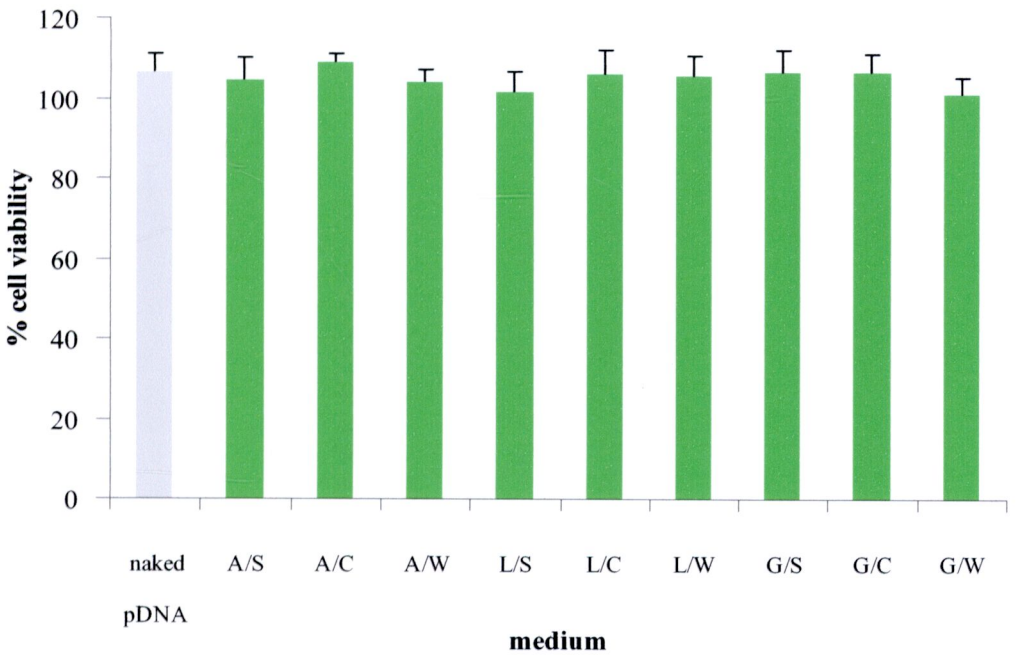

Figure 21 % Cell viability of HeLa cells incubated with medium of selected formulations (mean±SD, n=3). A, acetic acid; L, lactic acid; G, glycolic acid; S, sodium sulfate; C, sodium chloride; W, water.

Figure 21 shows that % cell viability of HeLa cells incubated with medium of selected formulation was nearly 100%, which equal to that of negative control. The result indicated that the medium of selected formulation was not toxic to the cells. Because of the hazard of acetic acid (Bullock et al., 2000), lactic acid and glycolic acid were selected to improve the safe gene delivery. Acetic acid is corrosive and irritating to the mucous membrane. It can cause damage to the digestive system and potentially lethal change in the acidity of the blood. While lactic acid is the substance in the body producing during normal metabolism and exercise and glycolic acid is non-toxic and it can enter the tricarboxylic acid cycle after which it is excreted as water and

carbondioxide. Therefore these two acids were used. However, since the concentration of the acid used in the study was only 5 mM, thus all of acids were not affect the viability of HeLa cells. Sodium sulfate and sodium chloride are the commonly used buffers. Therefore these two substances did not affect the viability of HeLa cells either.

7.3 Cell viability of HeLa cells incubated with the nanoparticles of the selected formulations and Lipofectamine™-pDNA complexes

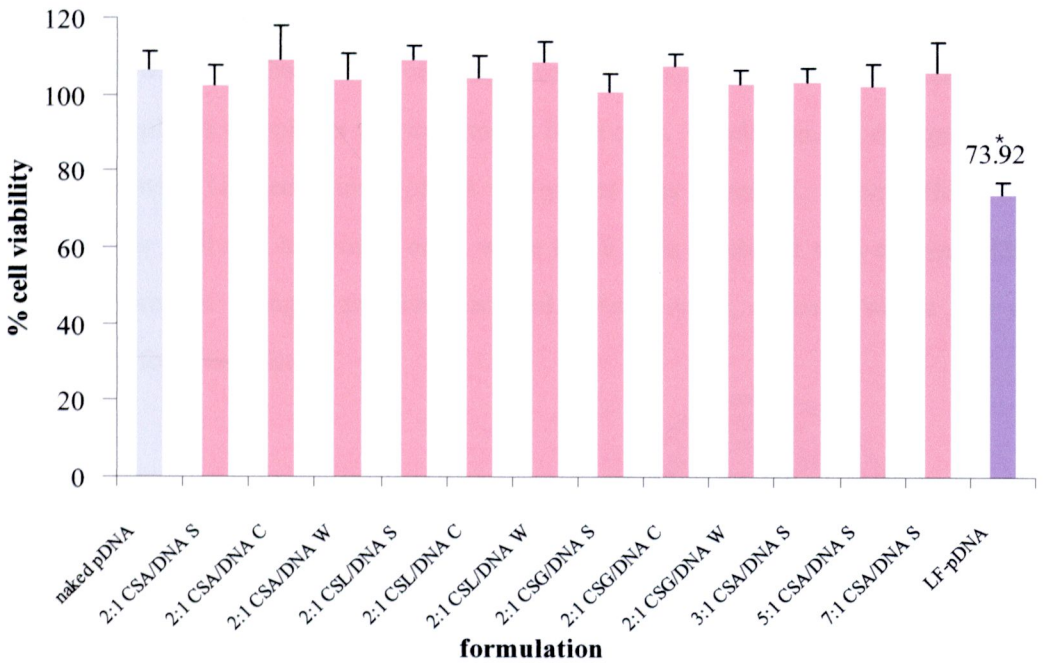

Figure 22 % Cell viability of HeLa cells incubated with the nanoparticles of selected formulations and Lipofectamine™-pDNA complexes (mean±SD, n=3). Differences values were statistically significant (*P<0.05). CSA, nanoparticles formulated with chitosan in acetic acid; CSL, nanoparticles formulated with chitosan in lactic acid; CSG, nanoparticles formulated with chitosan in glycolic acid; DNA S, nanoparticles formulated with pDNA in sodium sulfate; DNA C, nanoparticles formulated with pDNA in sodium chloride; DNA W, nanoparticles formulated with pDNA in water; LF-pDNA, Lipofectamine™-pDNA complexes.

Figure 22 shows that % cell viability of HeLa cells incubated with the nanoparticles of selected formulation was nearly 100%, which equal to that of negative control. The result indicated that nanoparticles of selected formulations did not affect the viability of HeLa cells, while % cell viability of HeLa cells incubated with Lipofectamine™-pDNA complexes was 73.92%, which was significantly different from each other. The result indicated that nanoparticles of selected formulation were safer than Lipofectamine™-pDNA complexes.

Cell viability study demonstrated that chitosan in the concentration range of 2-25 μg/ml in all medium of chitosan, which covered the concentration of chitosan used in the *in vitro* transfection efficiency study, media of selected nanoparticles and the nanoparticles of selected formulations did not affect the viability of HeLa cells. In contrast, Lipofectamine™ reagent and Lipofectamine™-pDNA complexes was toxic to the HeLa cells. In addition, the change of HeLa cells incubated with Lipofectamine™-pDNA complexes was observed. Some HeLa cells detached from the well and had rough edge, while HeLa cells incubated with chitosan-pDNA nanoparticles were not changed as aforementioned. As a result, chitosan was a safe and promising vector for gene delivery.